

## FLEXIBLE THIN-FILM RECHARGEABLE LITHIUM BATTERY

*J.F. Ribeiro<sup>1\*</sup>, R. Sousa<sup>1</sup>, J.A. Sousa<sup>1</sup>, L.M. Goncalves<sup>1</sup>, M.M. Silva<sup>2</sup>, L. Dupont<sup>3</sup> and J.H. Correia<sup>1</sup>*

<sup>1</sup>Algoritmi Centre, University of Minho, Guimarães, Portugal

<sup>2</sup>Chemistry Centre, University of Minho, Braga, Portugal

<sup>3</sup>LRCS – UMR 6007, Université de Picardie Jules Verne, Amiens, France

### ABSTRACT

Flexible thin-film rechargeable lithium battery was fabricated only by PVD techniques. The Kapton® substrate provides flexibility to the battery and at the same time supports the depositions conditions inside the vacuum chamber. Platinum and titanium were deposited by e-beam and used as cathode and anode current collectors of the battery, respectively. LiCoO<sub>2</sub> cathode was deposited by rf-sputtering with 150 W of power source, 40 sccm of Ar and 300 °C in the substrate during deposition. The electrolyte LiPON was also deposited by rf-sputtering and the conditions explained before in J. F. Ribeiro, *et al.*, [1]. The anode, lithium, was deposited with 3 μm thickness by thermal evaporation.

The open circuit potential, Nyquist diagrams and charge/discharge capacity were used for battery characterization. The modelling of Nyquist equivalent circuit allowed calculating some battery parameters, like, internal resistance, battery charge resistance and battery effective diffusion coefficient. The equivalent circuit and the parameters were calculated with the help of Zview™ software.

### KEYWORDS

Flexibility, thin-films, lithium batteries, Kapton®, equivalent circuit

### INTRODUCTION

Research in batteries has an exponential increase in the last decade, with a large amount of different applications, from planes to cars, laptops, cellular phones, and wireless sensors [2, 3]. Batteries are usually seen as the heaviest and costliest devices because, although there are simple in concept, their development is being much slower than the other electronic devices [2]. A great development in microelectronic industry, with even small electronic devices and consequently small power consumption, led to an increase in the attempts to develop even small microsystems [4]. The microsystems research led to an even more ambitious task of making them autonomous. Consequentially, the inclusion of harvesting modules (*e. g.* solar cells, thermoelectric and piezoelectric) to create an autonomous microsystems led to an increase of research in devices to storage energy and provides it to the microsystems when the energy source is not available [5]. Batteries is the natural choice for this task, because allows the energy storage and the levelling of energy from harvesting modules, that often suffer from current peaks.

Button and polymer li-ion batteries were the first choice for autonomous microsystems [5], but the limitations in size, security and energy density lead to an increase research in thin-film batteries. Thin-film battery technologies stand from the others because allows the use of only completely solid materials, which increase the security, because no leaking or explosion could occur [5]. This technology also allows a faster charge/discharge when compared with the conventional batteries [6]. These all-solid-state batteries can be fabricated only with physical vapour depositions (PVD) techniques [5, 6], making this batteries incredibly small, with only a few micrometres in thickness. Lithium phosphorous oxynitride (LiPON) thin-films are one of the most important materials for thin-film batteries [5]. The LiPON electrolyte is usually deposited by rf sputtering and allows the fabrication of all battery only with PVD techniques [1, 5, 6]. The thin-film technologies also allow a bigger energy density, as demonstrated in figure 1, because, since all materials all solid, the packaging of batteries can be much more light and small.

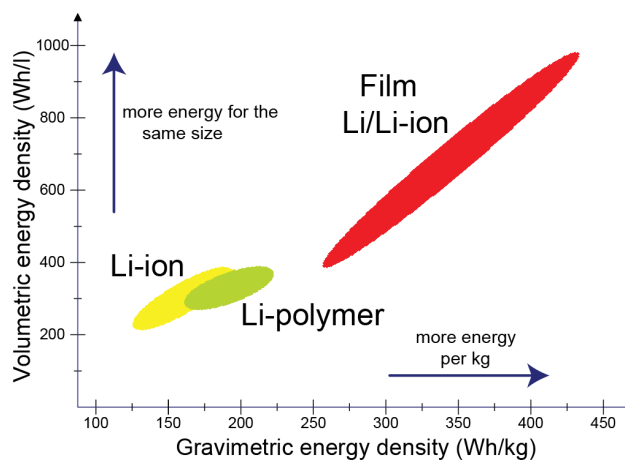


Figure 1: Battery capacity compared for different technologies [7].

The main objective of the work presented here is to develop a flexible and rechargeable thin-film lithium battery to use in autonomous and flexible microsystems. A different approach, when compared with the approach developed by G. Dennler, *et al.*, [3], was taken in this work. The possible fabrication of thin-film battery in the same substrate of the whole microsystem, allows getting an even thinner and light autonomous microsystem.

## FABRICATION

The design of thin-film lithium battery is presented in figure 2 and the fabrication process used shadow masks to pattern the presented layers. The substrate is an electrical insulator polyimide film named Kapton® 500HN with 127  $\mu\text{m}$  thickness, commercialized by DuPont™ [8]. Kapton® was successful used before by our group [9] and presents flexibility and temperature performance as the more important features [4].

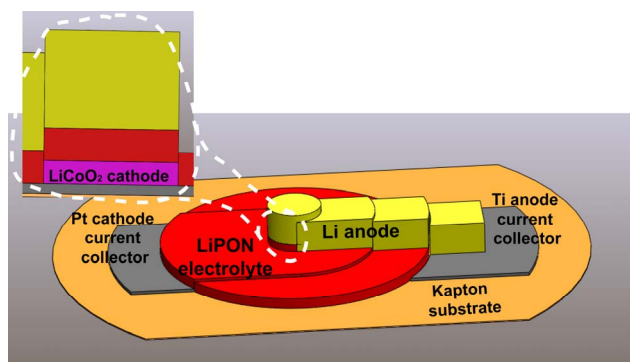


Figure 2: Design of thin-film battery with materials indication (not on scale for better visualization).

The platinum and titanium contact layers were deposited by e-beam with thickness of 0,2  $\mu\text{m}$ . These contacts are used interface electronic current from cathode and anode to ionic current inside the battery, but at same time, avoid reacting with it. The lithium cobalt oxide ( $\text{LiCoO}_2$ ) cathode was fabricated by RF sputtering with power source of 150 W, deposition pressure of  $3 \times 10^{-3}$  mbar, Ar flow of 40 sccm and with a heated substrate temperature of 300  $^\circ\text{C}$  during deposition. A deposition rate of 3,2  $\text{\AA}/\text{s}$  and a thickness of 0,7  $\mu\text{m}$  was obtained. The lithium phosphorous oxynitride (LiPON) electrolyte was fabricated by RF sputtering and results were published before by our group [1]. The metallic lithium anode was deposited by thermal evaporation, with 3  $\mu\text{m}$  thickness.

The table 1 presents a resume of the PVD techniques used and the thickness of each thin-film. The battery total thickness is about 4,9  $\mu\text{m}$  plus the 127  $\mu\text{m}$  from Kapton® substrate. The necessity of a protective layer to use battery outside the vacuum chamber [7] should increase the battery total thickens in a few micrometres.

Table 1: Materials deposited in battery fabrication with indication of the PVD technique and the thickness.

Material	PVD technique	Thickness ( $\mu\text{m}$ )
Pt	e-beam	0,2
Ti		
$\text{LiCoO}_2$	rf sputtering	0,7
LiPON		
Li	thermal evaporation	3
<b>Thin-film battery</b>	-	<b>4,9 (thin-films) + 127 (substrate)</b>

## RESULTS AND DISCUSSION

The battery characterization has started immediately after lithium deposition and without breaking vacuum, to avoid reaction of battery with air ( $\text{N}_2/\text{H}_2\text{O}/\text{O}_2$ ), since any protection was deposited [7]. Gamry Reference 600TM potentiostat/galvanostat was connected through feedthroughs, allowing the characterization of battery inside the vacuum chamber. All measurements was performed with the working electrode connected to cathode current collector (platinum) and the reference and counter electrode connected to anode current collector (titanium).

An open circuit potential (OCP) was the first measurement performed in the thin-film battery. A huge self-discharge current was immediately detected by the fast decrease of potential. The figure 3 shows the OCP just after the lithium deposition with a pronounced fading of approximately 9 mV in 30 s. This self-discharge was not expected due to well know negligible self-discharge of thin-film batteries [6]. The huge self-discharge was related to a possible thinner electrolyte (LiPON) in some area between the cathode and the anode. The OCP voltage of 2,39 V measured just after the lithium deposition also indicates an amorphous  $\text{LiCoO}_2$  [10]. After the first charge/discharge cycle, the thin-film battery fading appears to improve to approximately 8 mV in 30 s. This is connected to the creation of interface layers between the cathode/electrolyte and the electrolyte/anode [11]. After ten cycles of charge/discharge, the battery was completely destroyed, presenting a potential of 1,22 V and 53 mV lost in 30 s.

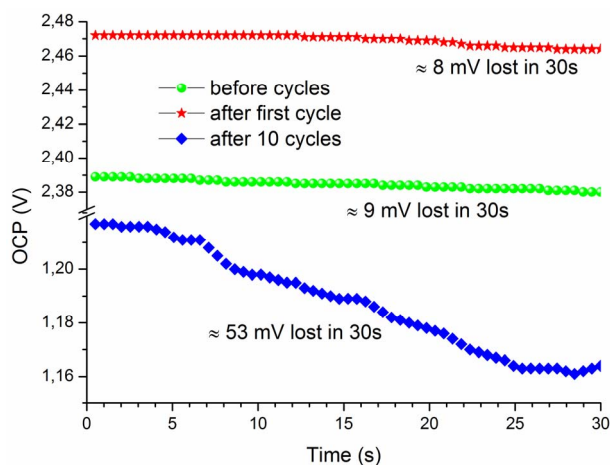


Figure 3: Open circuit potential of the battery before and after charge/discharge cycles.

Nyquist diagrams (figure 4) were traced applying a sinusoidal voltage of 10 mV AC in a range of 5 mHz to 200 kHz to the battery contacts. The Nyquist diagram was modelled with the typical equivalent circuit also presented in figure 4, which reflects the capacitor function of electric double layer and its barrier effect on electron transference from electrochemical polarization process and the Warburg impedance from concentration polarization processes.

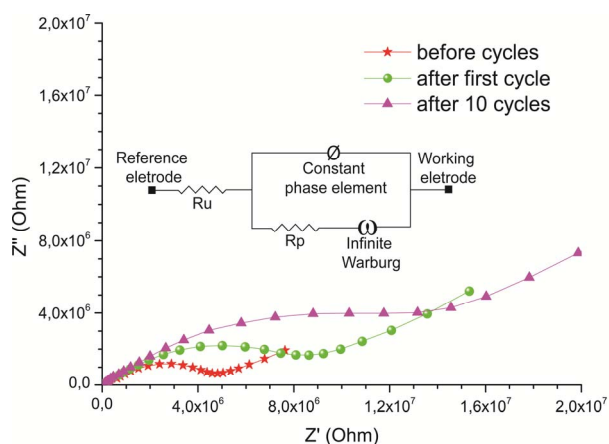


Figure 4: Nyquist diagrams representing complex impedance of the battery, before and after charge/discharge cycles and equivalent circuit obtained by approximation of Nyquist diagrams.

The equivalent circuit was modelled by mean of ZView™ software version 3.3c supplied by Scribner Associates Inc. company [12] and the effective diffusion coefficient (D) of the lithium ions calculate with equation 1 [13].

$$D = L^2/Wa-T \quad (1)$$

The L in equation 1 is the effective diffusion thickness and Wa-T is the Warburg coefficient. The other parameters calculated by the software are presented in table 2. The Ru represents the internal resistance of battery, the Rp represents the charge resistance, the Wa-R is Z' at very low frequency and the Wa-P is an exponent part and is set to 0,5 for finite length Warburg.

Table 2: Equivalent circuit parameters before the cycling, after first cycle and after 10 cycles. This parameters were provided by Zview™ software.

		Before cycles	After first cycle	After 10 cycles
	<b>Ru (kΩ)</b>	42,38	26,10	23,47
	<b>Rp (MΩ)</b>	4,98	9,54	15,98
<b>Warburg</b>	<b>Wa-R (MΩ)</b>	4,33	5,27	18,83
	<b>Wa-T</b>	17,45	5,76	13,27
	<b>Wa-P</b>	0,51	0,56	0,49
<b>CPE</b>	<b>CPE-T (e<sup>-8</sup>)</b>	1,18	1,07	1,13
	<b>CPE-P</b>	0,54	0,54	0,53
	<b>D (e<sup>-12</sup>)</b>	1,27	3,83	1,67

The internal resistance decreases with the course of cycling, especially after first cycle. This is related to the formation of the interface layers already mentioned before in this paper. On the contrary the charge resistance increase with the course of cycles and also has the bigger difference after first cycle. Effective diffusion (D) increases after the first cycle and starts to decrease after. All the parameters from Zview™ software have less than 10% of error.

The battery capacity during charge and discharge is presented in figure 5. These curves were obtained by repetitive chronopotentiometry during 10 cycles. The charge (figure 5 a)) was performed applying a current of 10 nA to the battery, until a voltage of 3.9 V was achieved. The discharge was realized by a current of -10 nA (figure 5 b)). The comparison between the charge and discharge capacity indicates an approximately four times lower capacity during discharge, which confirm the huge self-discharge current. A bad capacity retention is also notice, because of the difference between the voltage in the end of charge, 3,9 V and the beginning of discharge, 3,4 V. This difference is linked to the possible amorphous state of LiCoO<sub>2</sub> and consequently bad electrochemical performance of the battery [14].

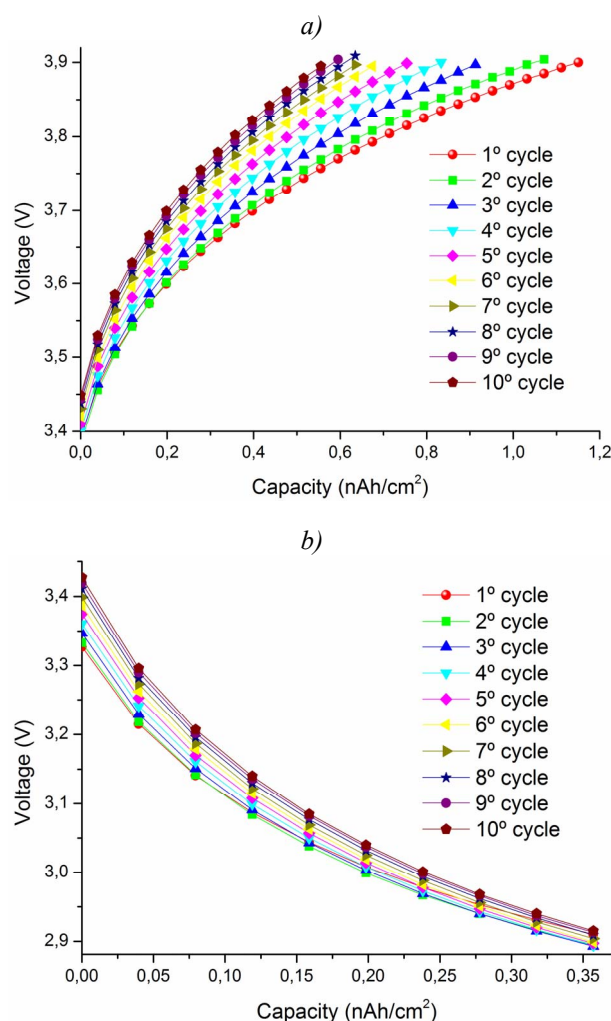
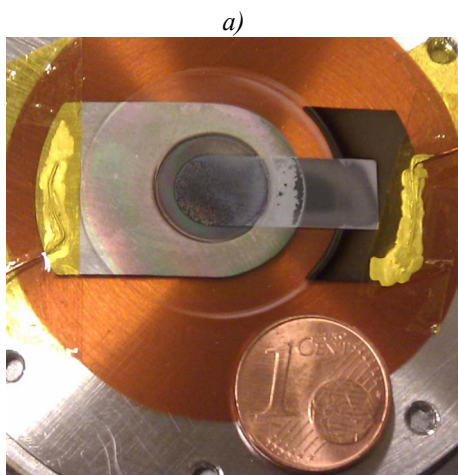


Figure 5: Capacity of the battery by square centimeter during charge (a) and discharge (b).

A capacity of 10,8 nAh was measured but with retention fading along charge/discharge cycles. Despite the low capacity, a battery was developed on a flexible substrate using only microelectronic well-known fabrication processes. The flexible and rechargeable thin-film lithium battery outlook and size is presented in figure 6 a) and b).



b)

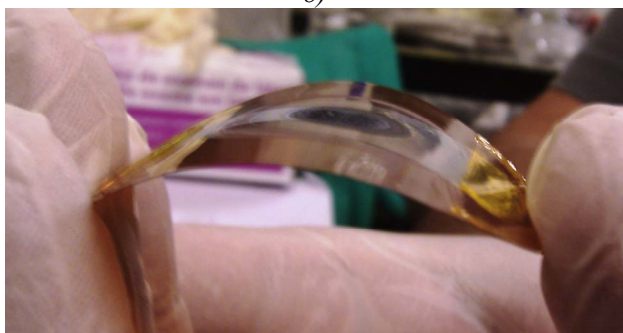


Figure 6: Photographs of flexible thin-film rechargeable lithium battery: a) top view with size indication; b) side view with flexibility demonstration.

## CONCLUSIONS

A thin-film flexible battery was successfully fabricated only with PVD techniques. A plastic Kapton® substrate with 127 µm thickness was utilized to endure the deposition conditions inside the vacuum chamber and provide flexibility to the battery. The battery was fabricated with Pt and Ti current collectors for cathode and anode, respectively. Both were deposited by e-beam. The cathode  $\text{LiCoO}_2$  was deposited by rf-sputtering with 0,7 µm thickness, Ar flow of 40 sccm and 300 °C in substrate during deposition. LiPON electrolyte was deposited under conditions published before by our group [1]. The anode, lithium, was deposited by thermal evaporation with 3 µm thickness.

The battery characterization was performed using OCP, Nyquist diagrams and charge/discharge capacity measurements during the battery cycling. An equivalent circuit was modelled with Nyquist diagrams using Zview™ software. This software allowed calculating of battery internal resistance, battery charge resistance, effective diffusion coefficient and other parameters. A huge self-discharge was measured and related to a possible thinner electrolyte in some area between the cathode and the anode. A low potential and retention fading along charge/discharge cycles were also measured and related to an amorphous  $\text{LiCoO}_2$ . Despite the capacity of 10,8 nAh, a battery was developed on a flexible substrate using only microelectronic well-known fabrication processes.

## ACKNOWLEDGEMENTS

This work was financially supported by FEDER/COMPETE and FCT funds with the project PTDC/EAAELC/114713/2009 and with first author scholarship SFRH/BD/78217/2011.

## REFERENCES

- [1] J. F. Ribeiro, *et al.*, "Enhanced solid-state electrolytes made of lithium phosphorous oxynitride films", *Thin Solid Films*, vol. 552, pp. 85-89, 2012.
- [2] M. Armand and J.-M. Tarascon, "Building better batteries", *Nature*, vol. 451, pp. 652-657, 2008.
- [3] G. Dennler, *et al.*, "A self-rechargeable and flexible polymer solar battery", *Solar Energy*, vol. 81, pp. 947-957, 2007.
- [4] L. Francioso, *et al.*, "Flexible thermoelectric generator for ambiente assisted living wearable biometric sensors", *Journal of Power Sources*, vol. 196, pp. 3239-3243, 2011.
- [5] B. Fleutot, *et al.*, "Characterization of all-solid-state Li/LiPONB/TiOS microbatteries produced at the pilot scale", *J. Power Sources*, vol. 196, pp. 10289-10296, 2011.
- [6] N. J. Dudney, "Solid-state thin-film rechargeable batteries", *Materials Science and Engineering B*, vol. 116, pp. 245-249, 2005.
- [7] J. F. Ribeiro, *et al.*, "Rechargeable lithium film batteries – encapsulation and protection", *Procedia Engineering*, vol. 47, pp. 676-679, 2012.
- [8] DuPont™ ©2011 Kapton® HN Polyimide Film Technical Data Sheet.
- [9] L. M. Goncalves, *et al.*, "Thermal co-evaporation of  $\text{Sb}_2\text{Te}_3$  thin-films optimized for thermoelectric applications", *Thin Solid Films*, vol. 519, pp. 4152-4157, 2011.
- [10] J. B. Bates, *et al.*, "Preferred orientation of polycrystalline  $\text{LiCoO}_2$  films", *Journal of The Electrochemical Society*, vol. 147, pp. 59-70, 2000.
- [11] B. Wang, *et al.*, "Characterization of thin-film rechargeable lithium batteries with lithium cobalt oxide cathodes", *Journal of The Electrochemical Society*, vol. 143, pp. 3203-3213, 1996.
- [12] <http://www.scribner.com/zplot-and-zview-for-windows.html>, accessed in 19-03-2013.
- [13] Z. P. Guo, *et al.*, "Synthesis of layered-structure  $\text{LiMn}_{1-x}\text{Cr}_x\text{O}_2$  by the Pechini Method and characterization as a cathode for rechargeable Li/LiMnO<sub>2</sub> cells", *Journal of The Electrochemical Society*, vol. 149, pp. A792-A795, 2002.
- [14] C. L. Liao and K. Z. Fung, "Lithium cobalt oxide cathode film prepared by rf sputtering", *Journal of Power Sources*, vol. 128, pp. 263-269, 2004.

## CONTACT

\*J.F. Ribeiro, tel: +351510190; jribeiro@dei.uminho.pt